Contribution from the Department of Chemistry and Molecular Structure Center, Indiana University, Bloomington, Indiana 47405

Crystal and Molecular Structure of $Al_2(O\text{-}t\text{-}Bu)_6$. Comments on the Extent of M–O π Bonding in Group 6 and Group 13 Alkoxides

Roger H. Cayton, Malcolm H. Chisholm,* Ernest R. Davidson,* Vincent F. DiStasi, Ping Du, and John C. Huffman

Received October 9, 1990

The reaction between $Al_2(NMe_2)_6$ and excess *t*-BuOH yields $Al_2(O\text{-}t\text{-}Bu)_6$, which crystallizes in the space group $P\bar{1}$ with $a = 9.946$ Å, $b = 9.755$ Å, $c = 16.332$ Å, $\alpha = 88.89°$, $\beta = 73.81°$, $\gamma = 88.89°$, and $Z = 2$. The molecule is pseudotetrahedral about each Al center and exhibits terminal Al–O bond lengths that are ca. 0.16 Å shorter than the sum of their atomic radii. The difference between the terminal Al–X bond lengths in Al_2Me_6 and $Al_2(O\text{-}t\text{-}Bu)_6$ amounts to 0.28 Å, the same bond length differential as found for the Mo–X distances in Mo_2R_6 and $Mo_2(OR)_6$ complexes. Both ab initio and Fenske–Hall-type MO calculations were performed on the model complexes $M_2(OH)_6$ (M = B, Al, Mo) in order to compare the M–O bonding in group 6 and group 13 alkoxides. For M = B and Al, the extent of M–O π bonding was found to be low and concentrated primarily on the terminal M–O interactions. The inclusion of Al 3d orbitals did not significantly increase the Al–O π bond orders. The ionic contribution calculated for the Al–O interactions was found to be significant and the major cause of the short Al–O distances. For M = Mo, the short Mo–O bond lengths were found to be the result of significant $O_{p\pi}$–$Mo_{d\pi}$ bonding, with less of an ionic contribution. Ab initio calculations were also performed on the model three-coordinate monomeric systems $H_2Al(OH)$, H_2AlMe, $H_2B(OH)$, and H_2BMe at the 6-31G* level. The optimized geometries showed the Al–O bond to be 0.28 Å shorter than the Al–C bond in these systems. The π bond orders were found to be only 0.26 for M = Al and 0.37 for M = B, indicating a significant degree of ionic character responsible for the short M–O bond lengths. Ab initio calculations on the model system H_4MoO showed a high degree of triple bond character in the Mo–O interaction.

Introduction

Alkoxides of the formula $M_2(OR)_6$ are known to adopt one of two structural types, I and II.[1] In I, alkoxide bridge formation allows maximum M–O bonding, while in II the preference for

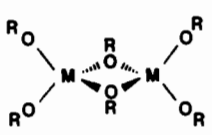

I

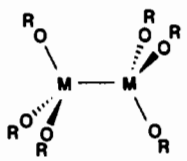

II

the unbridged structure reflects upon the important role of metal–metal bonding for the d^3 Mo^{3+} and W^{3+}. The latter is, of course, not possible for M = Al since it has a closed-shell configuration in its oxidation state of +3. Metal–metal and metal–ligand π bonding in transition-metal chemistry involves the use of $d\pi$ orbitals. For aluminum with configuration $3s^23p^1$, it is currently unfashionable to invoke significant Al d orbital participation, as indeed it is for Si and P in their complexes with coordination numbers greater than 4.[2] We report here the crystal and molecular structure of $Al_2(O\text{-}t\text{-}Bu)_6$, which, not surprisingly, is a member of the dimeric group of alkoxides of type I. This is, however, the first report of a structure for a homoleptic $[(Al(OR)_3)]_2$ compound[3] and allows a comparison of M–OR bonding in the series $M_2(OR)_6$ where M = Al, Mo, and W.

(1) M = Ce, R = $(t\text{-Bu})_2CH$, type I: Stecher, H. A.; Sen, A.; Rheingold, A. L. *Inorg. Chem.* **1989**, *28*, 3280. (b) M = Mo, R = CH_2-*t*-Bu, type II: Chisholm, M. H.; Cotton, F. A.; Murillo, C. A.; Reichert, W. W. *Inorg. Chem.* **1977**, *16*, 1801. (c) M = W, R = *i*-Pr, type II: Chisholm, M. H.; Clark, D. L.; Folting, K.; Huffman, J. C.; Hampden-Smith, M. J. *J. Am. Chem. Soc.* **1987**, *109*, 7750.

(2) For a related discussion of "the d-orbital problem" in the bonding in silicates, see: Janes, N.; Oldfield, E. *J. Am. Chem. Soc.* **1986**, *108*, 5743 and references therein. For π bonding in aluminum aryloxides, see: Healey, M. D.; Ziller, J. W.; Barron, A. R. *J. Am. Chem. Soc.* **1990**, *112*, 2949. Healy, M. D.; Wierda, D. A.; Barron, A. R. *Organometallics* **1988**, *7*, 2543. Lichtenberger, D. L.; Hogan, R. H.; Healy, M. D.; Barron, A. R. *J. Am. Chem. Soc.* **1990**, *112*, 3369. Power, M. B.; Bott, S. G.; Atwood, J. L.; Barron, A. R. *J. Am. Chem. Soc.* **1990**, *112*, 3446.

(3) A somewhat related Al_2(trisiloxide)$_2$ has recently been structurally characterized: Feher, F. J.; Budzichowski, T. A.; Weller, K. J. *J. Am. Chem. Soc.* **1989**, *111*, 7288. The structure of $[Al(O\text{-}i\text{-}Pr)_3]_4$ has also been reported: Turova, N. Ya.; Kozunov, V. A.; Yanovskii, A. I.; Bokii, N. G.; Struchkov, Yu. T.; Tarnopolskii, B. L. *J. Inorg. Nucl. Chem.* **1979**, *41*, 5.

Table I. Selected Bond Distances (Å) and Angles (deg for the $Al_2(O\text{-}t\text{-}Bu)_6$ Compound[a]

Bond Distances			
Al(1)–Al(1)*	2.7768 (23)	Al(1)′–O(12)′	1.681 (3)
Al(1)–O(2)	1.8243 (25)	O(2)–C(3)	1.474 (4)
Al(1)–O(2)*	1.8304 (26)	O(7)–C(8)	1.422 (4)
Al(1)–O(7)	1.6984 (27)	O(12)–C(13)	1.421 (4)
Al(1)–O(12)	1.6825 (27)	O(2)′–C(3)′	1.469 (4)
Al(1)′–Al(1)′*	2.7786 (23)	O(7)′–C(8)′	1.422 (4)
Al(1)′–O(2)′	1.8272 (26)	O(12)′–C(13)′	1.416 (4)
Al(1)′–O(2)′*	1.8309 (26)	C–C(methyl)	1.52 (1) (av)
Al(1)′–O(7)′	1.6895 (27)		
Bond Angles			
O(2)–Al(1)–O(2)*	81.11 (12)	O(7)′–Al(1)′–O(12)′	115.08 (14)
O(2)–Al(1)–O(7)	111.75 (12)	Al(1)–O(2)–Al(1)*	98.89 (12)
O(2)*–Al(1)–O(7)	109.75 (13)	Al(1)–O(2)–C(3)	129.72 (21)
O(2)–Al(1)–O(12)	116.37 (13)	Al(1)–O(2)*–C(3)*	130.88 (21)
O(2)*–Al(1)–O(12)	118.19 (13)	Al(1)–O(7)–C(8)	136.72 (24)
O(7)–Al(1)–O(12)	115.12 (13)	Al(1)–O(12)–C(13)	148.37 (23)
O(2)′–Al(1)′–O(2)′*	81.15 (12)	Al(1)′–O(2)′–Al(1)′*	98.85 (12)
O(2)′–Al(1)′–O(7)′	110.03 (13)	Al(1)′–O(2)′–C(3)′	130.39 (22)
O(2)′*–Al(1)′–O(7)′	111.22 (13)	Al(1)′–O(2)′*–C(3)′*	130.58 (22)
O(2)′*–Al(1)′–O(12)′	117.78 (14)	Al(1)′–O(7)′–C(8)′	140.24 (24)
O(2)′–Al(1)′–O(12)′	117.02 (13)	Al(1)′–O(12)′–C(13)′	152.60 (25)

[a] The two centrosymmetric and independent molecules are numbered with and without primes; an asterisk is used to identify an atom related by a center of symmetry to one already specified.

Results and Discussion

Molecular Structure of $Al_2(O\text{-}t\text{-}Bu)_6$. An ORTEP drawing of the $Al_2(O\text{-}t\text{-}Bu)_6$ molecule is given in Figure 1. Pertinent structural data and crystal data are given in Tables I and II, respectively. Atomic coordinates are listed in Table III.

The gross structural features of the molecule are not surprising. Coordination about each Al atom is pseudotetrahedral with the smallest O–Al–O angle being 81° associated with the bridging OR ligands. The central $Al_2(\mu\text{-}O)_2$ moiety is planar, and the molecule has a crystallographically imposed C_2 axis of symmetry. The Al–O–C groups associated with the terminal O-*t*-Bu ligands lie in a plane perpendicular to the $Al_2(\mu\text{-}O)_2$ moiety. The Al–O bridging distances are ca. 0.15 Å longer than the terminal Al–O bond distances.

Comparison of M–X Distances in M_2X_6 Compounds, Where M = Al and Mo and X = R and OR. The covalent radii of the metal atoms in M_2X_6 (M≡M) compounds, where M = Mo and W, can be reasonably estimated to be 1.38–1.40 Å with respect to metal–ligand bonding. For example, in M_2R_6 compounds[4] or M_2-

0020-1669/91/1330-1020$02.50/0

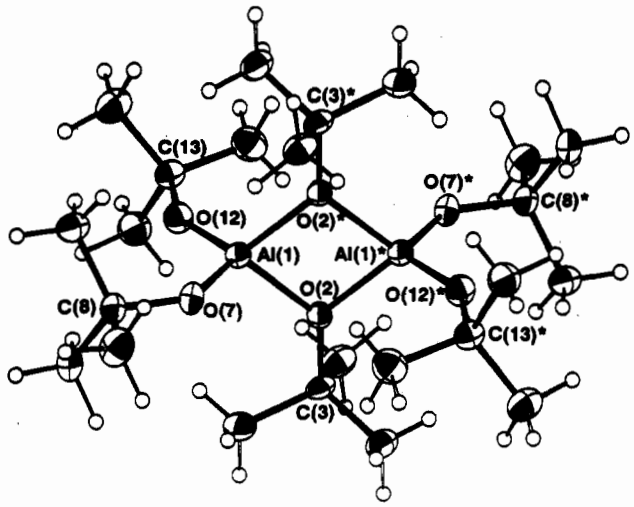

Figure 1. ORTEP drawing of one of the centrosymmetric $Al_2(O\text{-}t\text{-}Bu)_6$ molecules found in the unit cell, showing the number scheme used in the tables.

Table II. Summary of Crystal Data for $Al_2(O\text{-}t\text{-}Bu)_6$

empirical formula	$Al_2C_{24}H_{54}O_6$
color of crystal	colorless
crystal dimen, mm	0.25 × 0.25 × 0.25
space group	$P\bar{1}$
cell dimensions	
temp, °C	−155
a, Å	9.946 (3)
b, Å	9.755 (3)
c, Å	16.332
α, deg	88.89 (2)
β, deg	73.81 (1)
γ, deg	88.84 (1)
Z (molecules/cell)	2
vol, Å^3	1521.36
calcd density, gm/cm^3	1.083
wavelength, Å	0.71069
MW	492.65
linear absorption coeff, cm^{-1}	1.223
detector-to-sample dist, cm	22.5
sample-to-source dist, cm	23.5
av ω scan width at half-height	0.25
scan speed, deg/min	6.0
scan width, deg + dispersion	2.0
individual background, s	3
aperture size, mm	3.0 × 4.0
2θ range, deg	6–45
total no. of reflcns collected	5315
no. of unique intensities	3978
no. with $F > 0.0$	3652
no. with $F > 2.33\sigma(F)$	3227
$R(F)$	0.0552
$R_w(F)$	0.0578
goodness of fit for the last cycle	1.226
max δ/σ for the last cycle	0.35

$(OR')_4(R)_2$ compounds,[5] where R is an alkyl ligand bearing an α-carbon atom that is sp^3 hybridized, the M–C distances are in the range 2.14–2.17 Å. Given the commonly accepted covalent radius of C_{sp^3} as 0.77 Å, this places r_M in the range 1.37–1.40 Å. The M–OR distances are, however, notably shorter than those for M–C_{sp^3} and fall within the very narrow range of 1.88 (1) Å for all known $M_2(OR)_xY_{6-x}$ compounds where x = 6, 5, or 4 and Y is an alkyl, thiolate, or some other uninegative ligand. Although the covalent radius of oxygen sp^x where x = 1, 2, or 3 is less than that of the corresponding C_{sp^x} by ca. 0.1 Å, this alone cannot be

Table III. Fractional Coordinates and Isotropic Thermal Parameters for $Al_2(O\text{-}t\text{-}Bu)_6$

atom	10^4x	10^4y	10^4z	$10B_{iso}$, Å^2
Al(1)	6186 (1)	5738 (1)	4596 (1)	16
O(2)	4432 (2)	5444 (2)	4499 (1)	16
C(3)	3771 (4)	5865 (4)	3828 (2)	18
C(4)	4572 (5)	7086 (4)	3359 (3)	24
C(5)	2265 (4)	6257 (5)	4255 (3)	24
C(6)	3874 (5)	4679 (5)	3230 (3)	24
O(7)	6331 (3)	7335 (3)	4956 (2)	20
C(8)	7350 (4)	8382 (4)	4778 (3)	21
C(9)	6817 (5)	9502 (5)	5417 (3)	29
C(10)	7522 (5)	8939 (5)	3874 (3)	26
C(11)	8748 (5)	7792 (5)	4857 (3)	30
O(12)	7530 (3)	5226 (3)	3776 (2)	21
C(13)	8189 (4)	4163 (4)	3216 (2)	19
C(14)	8244 (5)	4628 (5)	2314 (3)	26
C(15)	9682 (4)	3975 (5)	3287 (3)	27
C(16)	7375 (5)	2848 (5)	3445 (3)	28
Al(1)′	6315 (1)	9594 (1)	9500 (1)	16
O(2)′	4475 (2)	9499 (2)	9509 (1)	17
C(3)′	3839 (4)	8958 (4)	8873 (2)	20
C(4)′	3952 (6)	10038 (5)	8183 (3)	34
C(5)′	2334 (5)	8644 (6)	9323 (3)	29
C(6)′	4647 (6)	7684 (5)	8510 (4)	36
O(7)′	7171 (3)	10683 (3)	8720 (2)	21
C(8)′	8464 (4)	10790 (4)	8075 (2)	20
C(9)′	8742 (5)	12309 (5)	7908 (3)	29
C(10)′	8325 (5)	10110 (6)	7277 (3)	31
C(11)′	9638 (5)	10104 (6)	8360 (3)	31
O(12)′	7174 (3)	8115 (3)	9575 (2)	25
C(13)′	7291 (4)	6810 (4)	9945 (3)	23
C(14)′	7581 (6)	5767 (5)	9252 (4)	36
C(15)′	8518 (5)	6852 (6)	10333 (4)	36
C(16)′	5932 (5)	6487 (5)	10630 (3)	33

Table IV. Estimated Bond Lengths from the Sum of Atomic Radii

bond	bond length, Å	bond	bond length, Å
Mo–C	2.15	Al–O	1.85
Mo–O	2.05	B–C	1.55
Al–C	1.95	B–O	1.45

held to account for the observed shortness of the M–OR distances. The availability of vacant dπ orbitals on the metal (those not used in forming the M–M triple bond) allows for $O_{p\pi}$-to-$M_{d\pi}$ bonding. This is indeed a commonly accepted phenomenum for early transition-metal alkoxide[6] and aryl oxide chemistry, and Rothwell and co-workers have very nicely tabulated M–OAr distances as a function of dπ electron count on the metal.[7]

The same degree of shortening exists in Al_2X_6 chemistry for X = OR relative to X = Me. The Al–C distance for the terminal methyl groups of Al_2Me_6 averages 1.97 Å,[8] and the Al–O distance for the terminal ligands of $Al_2(O\text{-}t\text{-}Bu)_6$ averages 1.69 Å. This represents a shortening of 0.28 Å in going from Al–C to Al–O, which is comparable to the difference between the M–C and M–O distances for M = Mo, W, (0.26–0.29 Å)! Table IV lists specific M–O and M–C bond lengths estimated by the sum of atomic radii.[8] Given that, at the current level of theoretical calculations, d orbital participation for Al is not taken to be significant, we feel this is a most interesting observation and one worthy of some general attention.

In an attempt to rationalize the observed shortness of the Al–O terminal bonds in $Al_2(O\text{-}t\text{-}Bu)_6$, we carried out both Fenske–Hall[9] and ab initio molecular orbital calculations on the model systems $M_2(OH)_6$. For the two techniques, calculations were performed both with and without the inclusion of d orbitals on Al.

(4) (a) M = Mo, R = CH_2SiMe_3: Huq, F.; Mowat, W.; Shortland, A.; Skapski, A. C.; Wilkinson, G. *J. Chem. Soc., Chem. Commun.* **1971**, 1079. (b) Chisholm, M. H.; Cotton, F. A.; Extine, M. W.; Stults, B. R. *Inorg. Chem.* **1976**, *15*, 2252.
(5) M = W, R = *t*-Bu, R′ = *i*-Pr: Chisholm, M. H.; Eichhorn, B. W.; Folting, K.; Huffman, J. C. *Organometallics* **1986**, *5*, 1599.
(6) (a) Chisholm, M. H. *Polyhedron* **1983**, *2*, 681. (b) Bradley, D. C.; Mehrotra, R. C.; Gaur, P. *Metal Alkoxides*; Academic Press: New York, 1972.
(7) Coffindaffer, T. W.; Steffy, B. D.; Rothwell, I. P.; Folting, K.; Huffman, J. C.; Streib, W. E. *J. Am. Chem. Soc.* **1989**, *111*, 4742.
(8) Vranka, R. G.; Amman, E. L. *J. Am. Chem. Soc.* **1967**, *89*, 3121.
(9) Hall, M. B.; Fenske, R. F. *Inorg. Chem.* **1972**, *11*, 768.
(10) Huffman, J. C.; Streib, W. *J. Chem. Soc., Chem. Commun.* **1971**, 911.

Table V. D_{2h} Optimized Geometries of $Al_2(OH)_6$ and $B_2(OH)_6$

	$Al_2(OH)_6$		$Al_2(CH_3)_6$	$B_2(OH)_6$
param[a]	6-31G	6-31G[b]	exptl[c]	6-31G*
$M-O_t$	1.681	1.704	1.97	1.396
$M-O_b$	1.852	1.839	2.14	1.547
O_t-M-O_t	119.4	119.7	105.0	97.7
$M-O_b-M$	100.6	100.9	123.0	119.4

[a] Bond lengths are in Å; bond angles are in deg. [b] d orbitals have been included in the basis set. [c] Experimental geometry, see ref 10.

Bonding Considerations. $Al_2(OH)_6$. The σ-bond framework of $Al_2(OH)_6$ can be described in terms of two isolated, tetrahedrally coordinated aluminum centers. The Al 3s and 3p orbitals are used to form the four Al–O σ interactions about each metal center. This leaves two sets of filled p orbitals on each of the terminal oxygen atoms and one filled p orbital on each bridging oxygen atom (oriented perpendicular to the plane of the Al_2O_2 core) to interact in a π fashion with the Al atoms. We will concentrate on these Al–O π interactions to elucidate their contributions to the seemingly short Al–O bond lengths.

The experimental geometry of $Al_2(O\text{-}t\text{-}Bu)_6$, idealized to D_{2h} symmetry, was used for the Fenske–Hall calculations on $Al_2(OH)_6$. In the case of the ab initio calculations, the geometry of $Al_2(OH)_6$ was optimized with the 6-31G basis set (i.e. no d orbitals included) to yield a D_{2h} geometry (see Table V). As is evident from Table V, the unusual 0.28 Å bond length shortening of the Al–O bonds relative to the Al–C bonds was reproduced computationally. Vibrational analysis of this geometry shows all positive eigenvalues, indicating a true minimum on the potential surface. With the constraint of D_{2h} symmetry, inclusion of d orbitals for the Al and O atoms in the 6-31G* basis set enhances the bonding of the cyclic Al–O bonds and slightly shortens their bond lengths by 0.013 Å. The terminal Al–O bonds were found to be lengthened by 0.023 Å.

At this point, we are in position to evaluate the extent of oxygen π donation to the aluminum p and d orbitals. A complete population analysis of $Al_2(OH)_6$, extracted from the results of both the Fenske–Hall and ab initio methods, is provided in Table VI. Without the inclusion of Al 3d orbitals, both techniques indicate only a modest degree of Al–O π interaction, and that occurring primarily in the *terminal* Al–O (Al–O_t) bonds. The Fenske–Hall results show a donation of 0.03 electrons from each O_t π orbital, an Al–O_t π overlap population of 0.04, and an Al–O_t π bond order of 0.09. By comparison, a pure covalent π interaction (e.g. that in ethylene) would exhibit a π bond order of 1.0. The ab initio results are comparable in most respects but do indicate a slightly greater overall Al–O π interaction. This is perhaps most evident in the higher Al–O π bond orders of 0.25 and 0.12 for the Al–O terminal and bridging interactions, respectively. As was mentioned above, the majority of the Al–O π bonding occurs with the terminal O atoms, for which two interactions are principally responsible. These are represented pictorially by III and IV. Both of these interactions can be viewed as a π donation from the O_t atoms into orbitals that are primarily Al–O_b (O_b = bridging oxygen) σ^* in character. That the terminal O-*t*-Bu ligands of $Al_2(O\text{-}t\text{-}Bu)_6$ are bent in a plane perpendicular to the Al_2O_2 core (see V) may be a reflection of the modest Al–O π interactions

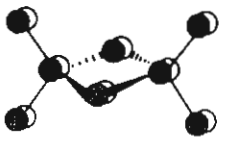

III

IV

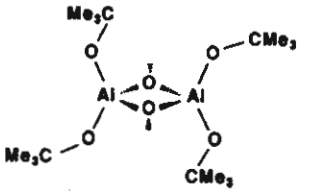

V

shown in III and IV, or simply the result of packing forces. These π interactions will be unaffected by alkoxide bending only if the bend occurs in the plane perpendicular to the Al_2O_2 core.

Not surprisingly, with the inclusion of Al 3d orbitals, the Al–O π bonding increases overall. The effect is most dramatic in the case of the Fenske–Hall technique (see Table VI), and as before the π bonding involves mainly the terminal Al–O interactions. This is clearly evident in the reduction of the O_t π orbital population from 1.97 to 1.87 electrons. It is also interesting to note that not only is there a significant $d\pi$–$p\pi$ bond order (0.27), but also the $p\pi$–$p\pi$ bond increases (0.16) when Al 3d orbitals are included. This phenomenon is likely due to d orbital participation in the Al–O σ bonds, thereby allowing the Al p orbitals to become more involved in π bonding. The ab initio results indicate less of an enhancement of the Al–O π bonding upon inclusion of d orbitals. The calculated $d\pi$–$p\pi$ bond order is 0.14, and the $p\pi$–$p\pi$ bond order actually decreases a small amount from 0.25 to 0.23. It is our conclusion that the Fenske–Hall method overestimates the Al 3d orbital participation in Al–O bonding, possibly due to the generation of overly diffuse virtual orbitals inherent within this technique. In any case, the degree of covalent Al–O π bonding calculated by either method is insufficient to account for the observed shortness of the Al–O bond lengths. We feel the lack of *covalent* π bonding is compensated for by an *ionic* contribution to the Al–O bond. The atomic charges of pertinent atoms are listed in Table VI and are fairly consistent between the two methods. The polarization of the Al–O bond reduces the degree of covalent π bond order possible but increases the strength of the ionic interaction.

It should also be noted that the Al–O_b bond distances, though longer than the Al–O_t bonds, are similarly short with respect to anticipations based on Al–C_b (C_b = bridging carbon) distances

Table VI. Population Analyses of $Al_2(OH)_6$ and $Mo_2(OH)_6$ as Calculated by Fenske–Hall and ab Initio Techniques

		Fenske–Hall			ab initio		
		$Al_2(OH)_6$			$Al_2(OH)_6$		
property	definition		*a*	$Mo_2(OH)_6$		*a*	$Mo_2(OH)_6$
total charge	M	+2.09	+1.24	+0.87	+2.05	+1.44	+1.56
	O_t	−0.95	−0.64	−0.52	−1.14	−0.93	−0.99
	O_b	−0.95	−0.59		−1.16	−0.96	
π population	O_t	1.97	1.87	1.79	1.92	1.90	1.82
	O_b	1.99	1.92		1.95	1.93	
π overlap	M–O_t	0.04	0.15	0.17	0.05	0.08	0.09
	M–O_b	0.00	0.07		0.02	0.03	
$p\pi$–$p\pi$ bond order	M–O_t	0.09	0.16	0.15	0.25	0.23	0.11
	M–O_b	0.00	0.06		0.12	0.08	
$d\pi$–$p\pi$ bond order	M–O_t		0.27	0.55		0.14	0.41
	M–O_b		0.14			0.09	
d population	M		0.76	4.19		0.36	3.89

[a] d orbitals have been included in the calculation.

Table VII. Population Analyses of $B_2(OH)_6$ and H_4MoO With the HF/6-31G* Wave Functions

property	definition	$B_2(OH)_6$ D_{2h}	H_4MoO C_{4v}
total charge	M	+0.83	+0.91
	O_t	−0.71	−0.71
	O_b	−0.77	
π population	O_t	1.89	1.64
	O_b	1.95	
π overlap	$M–O_t$	0.09	0.13
	$M–O_b$	0.02	
pπ–pπ bond order	$M–O_t$	0.26	0.24
	$M–O_b$	0.06	
dπ–pπ bond order	$M–O_t$	0.08	0.37
	$M–O_b$	0.06	
d populations	M	0.22	3.74

in Al_2Me_6. The Δ(Al–O/C) distance is 0.29 Å for both terminal and bridging bonds. Since there is relatively little $Al–O_b$ π bonding (half as much as for the terminal bonds, see Table VI), the shortening is most reasonably explained by the ionic contribution.

$Mo_2(OH)_6$. In order to address the validity of such an argument, we undertook comparative calculations on the related model system $Mo_2(OH)_6$. It should be remembered that a similar degree of shortening was observed between the M–C and M–O bonds for both M = Al and Mo.

Identical geometries were used for both the Fenske–Hall and ab initio calculations of $Mo_2(OH)_6$, with the calculational details listed in the Experimental Section. The bonding in $Mo_2(OH)_6$ has been described in detail elsewhere;[11] therefore here we will concentrate only upon a comparison of the Mo–O and Al–O π bonding. The population analysis of $Mo_2(OH)_6$ is provided in Table VI for the Fenske–Hall and ab initio methods. Once again the results of the two methods are quite consistent. Not surprisingly, the net Mo–O covalent π bonding is greater than that found for the Al–O interactions. Most indicative is the relatively large dπ–pπ bond order, calculated to be 0.55 via Fenske–Hall and 0.41 via ab initio. This increased covalent Mo–O π bond order is accompanied by a less ionic Mo–O bond as compared to the $Al_2(OH)_6$ system. Therefore, the "short" M–O bonds of $Al_2(OH)_6$ and $Mo_2(OH)_6$ appear to be due to a high degree of ionic character in the former case and a high degree of covalent π bonding in the latter case. That the very same extent of M–O bond shortening is observed for both systems would seem to be fortuitous. To more fully investigate the nature of the M–O π bonding in related systems, we examined a series of compounds via ab initio calculations.

$B_2(OH)_6$. Since the 3d orbitals of boron are quite high in energy and much less accessible for metal–ligand bonding, compared to aluminum, we chose to compare the model systems $B_2(OH)_6$ and $Al_2(OH)_6$. The geometry of $B_2(OH)_6$ was optimized at the 6-31G* level under the constraint of D_{2h} symmetry, and the resulting parameters are listed in Table V. A population analysis of $B_2(OH)_6$ (see Table VII) confirms the reduced participation of the 3d orbitals in M–O π bonding compared with that in $Al_2(OH)_6$. However, the degree of M–O pπ–pπ bonding is similar for both $B_2(OH)_6$ and $Al_2(OH)_6$, and as for $Al_2(OH)_6$, the terminal B–O bonds exhibit the greater degree of π bonding. The major difference between the two systems resides in the ionic character of the M–O bonds. The B–O bonds are found to be significantly more covalent than the corresponding Al–O bonds, a trend that would seem consistent on the basis of the relative electronegativities of B and Al.

$H_2Al(OH)$, H_2AlMe, $H_2B(OH)$, and H_2BMe. Since the aluminum atoms in $Al_2(OH)_6$ are four-coordinated, there are no orbitals free to participate solely in Al–O π bonding. As we demonstrated earlier, the Al–O π bonding in $Al_2(OH)_6$ occurs primarily through donation into Al–O σ* orbitals. We felt it instructive to compare this type of M–O π bonding with molecules capable of exhibiting a pure M–O π bond. The three-coordinate complexes $H_2Al(OH)$ and $H_2B(OH)$ contain an empty p orbital on the metal into which the O atoms may donate electron density in a π fashion. Furthermore, calculations on the molecules H_2AlMe and H_2BMe will allow a direct comparison to be drawn between M–C and M–O bonding in these three-coordinate species.

Table VIII. HF/6-31G* Optimized Bond Length and Population Analyses of $H_2Al(OH)$, H_2AlMe, $H_2B(OH)$, and H_2BMe under the Constraint of C_s Symmetry

property	definition	$H_2Al(OH)$	H_2AlMe	$H_2B(OH)$	H_2BMe
R, Å	M–O(C)	1.697	1.972	1.344	1.576
total charge	M	+0.83	+0.70	+0.29	+0.28
	O(C)	−0.93	−0.94	−0.61	−0.81
π population	O(C)	1.87	1.12	1.79	1.12
π overlap	M–O(C)	0.09	0.01	0.12	0.02
pπ–pπ bond order	M–O(C)	0.26	0.04	0.37	0.08
dπ–pπ bond order	M–O(C)	0.10	0.02	0.06	0.02
d population	M	0.21	0.16	0.29	0.05

The geometry of these molecules was optimized under the constraint of C_s symmetry using 6-31G* wave functions. The overall structures are pictured in VI and VII, and the values

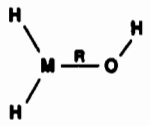

VI

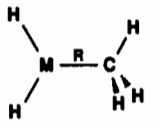

VII

determined for R are given in the top line of Table VIII. It is interesting to note that the bond length shortening of the Al–O bond compared to the Al–C bond in these monomers (0.275 Å) is about the same amount as that observed for the dimers.

Population analyses of these monomers are listed in Table VIII. Although the $H_2M(OH)$ complexes are capable of forming a pure M–O π bond, the pπ–pπ bond order was found to be only 0.26 for M = Al and 0.37 for M = B, again significantly less than 1.0. As before, the observed shortening appears to be a combination of covalent M–O π bonding and an ionic contribution. For both Al and B, d orbital participation was found to be quite low.

H_4MoO. H_4MoO represents a simple model to compare the contribution of d orbitals to Mo–O π bonding with that of p orbitals. The geometry of H_4MoO was optimized with C_{4v} symmetry to yield the parameters shown in VIII. The population

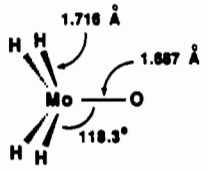

VIII

analysis on H_4MoO (see Table VII) shows a larger Mo–O dπ–pπ bond order (0.37) than pπ–pπ bond order (0.24). This is consistent with the empty $4d_{xz}$ and $4d_{yz}$ orbitals being lower in energy than the $5p_x$ and $5p_y$ orbitals. The total π bond order of 0.61 (for one of the two M–O π interactions) indicates that the M–O bond has significant triple bond character.

Conclusions

Through a combination of Fenske–Hall and ab initio methods we have been able to compare the M–O interactions in a series of main-group and transition-metal complexes. The short Al–O distances in $Al_2(OH)_6$ were found to be the result of a small amount of covalent π bonding and a significant ionic contribution to the Al–O interactions. Furthermore, the Al 3d orbitals were found to contribute little to the Al–O π bonding. By comparison, the equally short Mo–O distances in $Mo_2(OH)_6$ appear to be due in greater part to covalent Mo–O π bonding, employing primarily the Mo 4d orbitals, with less contribution from ionic character.

(11) (a) Cotton, F. A.; Stanley, G. G.; Kalbacher, B. J.; Green, J. C.; Seddon, E. A.; Chisholm, M. H. *Proc. Natl. Acad. Sci. U.S.A.* **1977**, *74*, 3109. (b) Bursten, B. E.; Cotton, F. A.; Green, J. C.; Kalbacher, B. J. *J. Am. Chem. Soc.* **1980**, *102*, 4579.

The key observation is that bond length and π bond order do not necessarily correlate. A very short metal oxygen bond may result from a high degree of ionic character or alternatively from multiple bonding, $O_{p\pi}$ to $M_{d\pi}$. In any event the π bond order is likely to be less than might be anticipated by simple considerations of orbital availability because of the differences in electronegativities. Thus, the less electropositive metals in their highest oxidation states, e.g. Os^{8+} would be expected to have the highest π bond order though their M–O distances may not be shorter than those involving a more electropositive metal, e.g. Zr^{4+}, which would have more ionic character.

Experimental Section

Computational Procedures. Molecular orbital calculations were performed at the Indiana University Computational Chemistry Center. All atomic wave functions used in the Fenske–Hall calculations were generated by using the method of Bursten, Jensen, and Fenske.[12] Contracted double-ζ representations were used for the Mo 4d, Al 3p, and O 2p AO's. The MO 5s and 5p exponents were fixed at 2.20, and the Al 3d component was fixed at 1.3552. All calculations were converged with a self-consistent-field iterative technique by using a convergence criteria of 0.0010 as the largest deviation between atomic orbital populations for successive cycles. The atomic parameters of the model complex $Al_2(OH)_6$ were taken from the X-ray structure data given in this work and idealized to D_{2h} symmetry with Al–O–H angles set to 180°. The model complex $Mo_2(OH)_6$ was constructed with D_{3d} symmetry, assuming the following atomic parameters: Mo–Mo = 2.22 Å, Mo–O = 1.88 Å, O–H = 0.96 Å, Mo–Mo–O = 106°, and Mo–O–H = 180°.

The geometry and vibrational frequencies of $Al_2(OH)_6$, $B_2(OH)_6$, $H_2Al(OH)$, H_2AlMe, $H_2B(OH)$, and H_2BMe were determined at the RHFSCF level, using the Gaussian 86 programs.[13] Population analyses were performed with the MELDF package of programs.[14]

For the ab initio calculations on $Mo_2(OH)_6$ and H_4MoO, an effective core potential[15] was used for the Mo atom. The 4s, 4p, 4d, and 5s electrons of Mo were treated explicitly with a Gaussian basis set of multiple ζ. For $Mo_2(OH)_6$ a single-point calculation was performed at the geometry described above for the Fenske–Hall calculation. For H_4MoO, single-point RHFSCF calculations at 10 geometries with various Mo–O and Mo–H bond lengths and O–Mo–H bond angles were carried out. The optimized geometry was found from a quadratic fit of these three parameters from the 10 points calculated.

$Al_2(O\text{-}t\text{-}Bu)_6$ was synthesized by the reaction between $Al_2(NMe_2)_6$ and t-BuOH (excess) in benzene. Crystals suitable for an X-ray study were obtained from toluene solution.

X-ray Structural Determination. General operating procedures have been described.[16]

$Al_2(O\text{-}t\text{-}Bu)_6$. A summary of crystal data is given in Table II. A suitable crystal was located and transferred to the goniostat by using inert atmosphere handling techniques and cooled to −155 °C for characterization and data collection.

A systematic search of a limited hemisphere of reciprocal space located a set of diffraction maxima with no symmetry or systematic absences, indicating a triclinic space group. Subsequent solution and refinement of the structure confirmed the centrosymmetric choice, $P\bar{1}$. It is noted that a "pseudomonoclinic" cell exists. Careful examination of the data indicates that the symmetry is accidental.

Data were collected in the usual manner using a continuous θ–2θ scan with fixed backgrounds. Data were reduced to a unique set of intensities and associated σ in the usual manner. The structure was solved by a combination of direct methods (MULTAN78) and Fourier techniques. All hydrogen atoms were clearly visible in a difference Fourier synthesis phased on the non-hydrogen parameters. All hydrogen atoms were refined isotropically and non-hydrogen atoms anisotropically in the final cycles.

There are two independent molecules, each at a center of inversion. The molecules are essentially identical.

A final difference Fourier was featureless, with the largest peak being 0.36 e/Å^3.

Atomic coordinates are given in Table III.

Acknowledgment. We thank the National Science Foundation for support. R.H.C. is a National Science Foundation Postdoctoral Fellow.

Supplementary Material Available: For $Al_2(O\text{-}t\text{-}Bu)_6$, tables of anisotropic thermal parameters and bond distances and angles and figures showing stereoviews and structures with the atom numbering schemes at two different rotations (6 pages); a listing of structure factors for $Al_2(O\text{-}t\text{-}Bu)_6$ (9 pages). Ordering information is given on any current masthead page.

(12) Bursten, B. E.; Jensen, J. R.; Fenske, R. F. *J. Chem. Phys.* **1978**, *68*, 3320.
(13) Frisch; et al. *Gaussian 86*; Carnegie-Mellon Quantum Chemistry Publishing Unit, Carnegie-Mellon University: Pittsburgh, PA, 1986.
(14) The MELDF collection of electronic structure codes were developed by L. E. McMerchie, S. T. Elbert, S. R. Langhoff, and E. R. Davidson and were extensively modified by D. Feller and D. C. Rallings.
(15) Hay, P. J.; Wadt, W. R. *J. Chem. Phys.* **1985**, *82*, 299.
(16) Chisholm, M. H.; Folting, K.; Huffman, J. C.; Kirkpatrick, C. C. *Inorg. Chem.* **1984**, *23*, 1021.